Self-trapped leaky waves in lattices: discrete and Bragg soleakons

Maxim Kozlov,* Ofer Kfir, and Oren Cohen

Solid state institute and physics department, Technion -Israel Institute of Technology, Haifa, 32000, Israel
**kozlov@tx.technion.ac.il*

Abstract: We propose lattice soleakons: self-trapped waves that self-consistently populate slowly-attenuating leaky modes of their self-induced defects in periodic potentials. Two types, discrete and Bragg, lattice soleakons are predicted. Discrete soleakons that are supported by combination of self-focusing and self-defocusing nonlinearities propagate robustly for long propagation distances. They eventually abruptly disintegrate because they emit power to infinity at an increasing pace. In contrast, Bragg soleakons self-trap by only self-focusing nonlinearity. Also, they do not disintegrate because they emit power at a decreasing rate.

OCIS codes: (190.5940) Self-action effects; (190.6135) Spatial solitons.

References and links

1. A. A. Ovchinnikov, "Localized long-lived vibrational states in molecular crystals," Zh. Exp. Theor. Phys. **57**, 263–270 (1969).
2. W. P. Su, J. R. Schrieffer, and A. J. Heeger, "Solitons in polyacetylene," Phys. Rev. Lett. **42**(25), 1698–1701 (1979).
3. A. J. Sievers and S. Takeno, "Intrinsic localized modes in anharmonic crystals," Phys. Rev. Lett. **61**(8), 970–973 (1988).
4. A. S. Davydov, "The theory of contraction of proteins under their excitation," J. Theor. Biol. **38**(3), 559–569 (1973).
5. W. Chen and D. L. Mills, "Gap solitons and the nonlinear optical response of superlattices," Phys. Rev. Lett. **58**(2), 160–163 (1987).
6. D. N. Christodoulides and R. I. Joseph, "Discrete self-focusing in nonlinear arrays of coupled waveguides," Opt. Lett. **13**(9), 794–796 (1988).
7. D. N. Christodoulides and R. I. Joseph, "Slow Bragg solitons in nonlinear periodic structures," Phys. Rev. Lett. **62**(15), 1746–1749 (1989).
8. J. Feng, "Alternative scheme for studying gap solitons in an infinite periodic Kerr medium," Opt. Lett. **18**(16), 1302–1304 (1993).
9. D. Mandelik, H. S. Eisenberg, Y. Silberberg, R. Morandotti, and J. S. Aitchison, "Observation of mutually trapped multiband optical breathers in waveguide arrays," Phys. Rev. Lett. **90**(25), 253902 (2003).
10. J. W. Fleischer, G. Bartal, O. Cohen, T. Schwartz, O. Manela, B. Freedman, M. Segev, H. Buljan, and N. K. Efremidis, "Spatial photonics in nonlinear waveguide arrays," Opt. Express **13**(6), 1780–1796 (2005).
11. M. Sato, B. E. Hubbard, and A. J. Sievers, "Colloquium: Nonlinear energy localization and its manipulation in micromechanical oscillator arrays," Rev. Mod. Phys. **78**(1), 137–157 (2006).
12. E. Kenig, B. A. Malomed, M. C. Cross, and R. Lifshitz, "Intrinsic localized modes in parametrically driven arrays of nonlinear resonators," Phys. Rev. E Stat. Nonlin. Soft Matter Phys. **80**(4), 046202 (2009).
13. E. Trías, J. J. Mazo, and T. P. Orlando, "Discrete breathers in nonlinear lattices: experimental detection in a josephson array," Phys. Rev. Lett. **84**(4), 741–744 (2000).
14. N. K. Efremidis and D. N. Christodoulidis, "Lattice solitons in Bose-Einstein condensates," Phys. Rev. A **67**(6), 063608 (2003).
15. B. Eiermann, Th. Anker, M. Albiez, M. Taglieber, P. Treutlein, K. P. Marzlin, and M. K. Oberthaler, "Bright Bose-Einstein gap solitons of atoms with repulsive interaction," Phys. Rev. Lett. **92**(23), 230401 (2004).
16. F. Bloch, "Über die quantenmechanik der elektronen in kristallgittern," Z. Phys. **52**, 555–600 (1928).
17. H. S. Eisenberg, Y. Silberberg, R. Morandotti, A. R. Boyd, and J. S. Aitchison, "Discrete spatial optical solitons in waveguide arrays," Phys. Rev. Lett. **81**(16), 3383–3386 (1998).
18. J. W. Fleischer, T. Carmon, M. Segev, N. K. Efremidis, and D. N. Christodoulides, "Observation of discrete solitons in optically induced real time waveguide arrays," Phys. Rev. Lett. **90**(2), 023902 (2003).
19. J. W. Fleischer, M. Segev, N. K. Efremidis, and D. N. Christodoulides, "Observation of two-dimensional discrete solitons in optically induced nonlinear photonic lattices," Nature **422**(6928), 147–150 (2003).
20. D. Neshev, E. Ostrovskaya, Y. Kivshar, and W. Krolikowski, "Spatial solitons in optically induced gratings," Opt. Lett. **28**(9), 710–712 (2003).

#191503 - $15.00 USD Received 30 May 2013; revised 15 Jul 2013; accepted 15 Jul 2013; published 14 Aug 2013

21. H. Martin, E. D. Eugenieva, Z. Chen, and D. N. Christodoulides, "Discrete solitons and soliton-induced dislocations in partially coherent photonic lattices," Phys. Rev. Lett. **92**(12), 123902 (2004).
22. A. Fratalocchi, G. Assanto, K. A. Brzdakiewicz, and M. A. Karpierz, "Discrete propagation and spatial solitons in nematic liquid crystals," Opt. Lett. **29**(13), 1530–1532 (2004).
23. D. Mandelik, R. Morandotti, J. S. Aitchison, and Y. Silberberg, "Gap solitons in waveguide arrays," Phys. Rev. Lett. **92**(9), 093904 (2004).
24. N. K. Efremidis, J. Hudock, D. N. Christodoulides, J. W. Fleischer, O. Cohen, and M. Segev, "Two-dimensional optical lattice solitons," Phys. Rev. Lett. **91**(21), 213906 (2003).
25. S. F. Mingaleev, Y. S. Kivshar, and R. A. Sammut, "Long-range interaction and nonlinear localized modes in photonic crystal waveguides," Phys. Rev. E Stat. Phys. Plasmas Fluids Relat. Interdiscip. Topics **62**(4 4 Pt B), 5777–5782 (2000).
26. O. Cohen, T. Schwartz, J. W. Fleischer, M. Segev, and D. N. Christodoulides, "Multiband vector lattice solitons," Phys. Rev. Lett. **91**(11), 113901 (2003).
27. A. A. Sukhorukov, Y. S. Kivshar, "Multigap discrete vector solitons," Phys. Rev. Lett. **91**(11), 113902 (2003).
28. H. Buljan, O. Cohen, J. W. Fleischer, T. Schwartz, M. Segev, Z. H. Musslimani, N. K. Efremidis, and D. N. Christodoulides, "Random-phase solitons in nonlinear periodic lattices," Phys. Rev. Lett. **92**(22), 223901 (2004).
29. O. Cohen, G. Bartal, H. Buljan, T. Carmon, J. W. Fleischer, M. Segev, and D. N. Christodoulides, "Observation of random-phase lattice solitons," Nature **433**(7025), 500–503 (2005).
30. O. Peleg, Y. Plotnik, N. Moiseyev, O. Cohen, and M. Segev, "Self-trapped leaky waves and their interactions," Phys. Rev. A **80**(4), 041801 (2009).
31. N. Moiseyev, P. R. Certain, and F. Weinhold, "Resonance properties of complex-rotated hamiltonians," Mol. Phys. **36**(6), 1613–1630 (1978).
32. H. C. Gurgov and O. Cohen, "Spatiotemporal pulse-train solitons," Opt. Express **17**(9), 7052–7058 (2009).
33. I. B. Burgess, M. Peccianti, G. Assanto, and R. Morandotti, "Accessible light bullets via synergetic nonlinearities," Phys. Rev. Lett. **102**(20), 203903 (2009).
34. O. Lahav, H. C. Gurgov, P. Sidorenko, O. Peleg, L. Levi, A. Fleischer, and O. Cohen, "Self-phase modulation spectral broadening in two-dimensional spatial solitons: toward three-dimensional spatiotemporal pulse-train solitons," Opt. Lett. **37**(24), 5196–5198 (2012).
35. S. Giovanazzi, A. Gorlitz, and T. Pfau, "Ballistic expansion of a dipolar condensate," J. Opt. B **5**(2), S208–S211 (2003).
36. A. Griesmaier, J. Stuhler, T. Koch, M. Fattori, T. Pfau, and S. Giovanazzi, "Comparing contact and dipolar interactions in a Bose-Einstein condensate," Phys. Rev. Lett. **97**(25), 250402 (2006).
37. A. W. Snyder and J. D. Love, *Optical Waveguide Theory* (Chapman & Hall, 1983).
38. A. R. Champneys, B. A. Malomed, and M. J. Friedman, "Thirring solitons in the presence of dispersion," Phys. Rev. Lett. **80**(19), 4169–4172 (1998).
39. J. Yang, B. A. Malomed, and D. J. Kaup, "Embedded solitons in second-harmonic-generating systems," Phys. Rev. Lett. **83**(10), 1958–1961 (1999).
40. J. Yang, "Fully localized two-dimensional embedded solitons," Phys. Rev. A **82**(5), 053828 (2010).
41. X. Wang, Z. Chen, J. Wang, and J. Yang, "Observation of in-band lattice solitons," Phys. Rev. Lett. **99**(24), 243901 (2007).
42. G. Agraval, *Nonlinear Fiber Optics*, 3rd ed. (Academic Press, 2001).

1. Introduction

Self-trapped states in periodic systems (lattices) are ubiquitous in nature and play a fundamental role in many branches of science, such as solid state physics (localized modes in crystals and conducting polymer chains) [1–3], biology (energy transfer in protein α-helices) [4], nonlinear optics (self-trapped beams and pulses of light in optical lattices) [5–10], mechanics (energy localization in oscillator arrays) [11, 12] and quantum mechanics (self-confined excitations in Josephson junction arrays and localized atomic Bose-Einstein condensates) [13–15]. Two types of self-trapped lattice states have been investigated: lattice solitons and lattice breathers. During evolution, the shape of lattice solitons is preserved while it oscillates in lattice breathers. Still, the wave-packets of both lattice solitons and lattice breathers exhibit exponential decay in the trapped directions. As a result, coherent interactions between lattice solitons or breathers are fundamentally short-range.

Self-trapped lattice waves can also be divided according to the location of their energies (or propagation constants) in the band structure. The linear modes of lattices are Floquet-Bloch waves, with their spectra divided into bands that are separated by gaps in which propagating modes do not exist [16]. The eigenvalues of a self-trapped lattice state can reside in the semi-infinite gap, in which case it is often termed discrete soliton [2, 4, 6] or discrete breather [1, 3, 13], or in a gap between two bands, hence termed gap [5, 8, 15] or Bragg soliton [7]. Notably, discrete and gap solitons often exhibit different properties because discrete solitons are trapped through total internal reflections whereas gap solitons are

#191503 - $15.00 USD Received 30 May 2013; revised 15 Jul 2013; accepted 15 Jul 2013; published 14 Aug 2013

localized by Bragg reflections [10]. A prime example for a system in which self-localized lattice waves have been investigated experimentally is optical nonlinear waveguide arrays [17–24]. Discrete solitons [17–22, 24], discrete breathers [25], gap solitons [23, 24] and gap breathers [9], as well as more complicated structures such as vector lattice solitons [26, 27] and incoherent lattice solitons [28, 29], have been explored in one and two dimensional arrays of waveguides.

Lattice solitons and lattice breathers have their counterparts in nonlinear homogeneous media. In homogeneous media, however, another type of self-localized particle-like waves was recently proposed: self-trapped leaky waves: soleakons [30]. A soleakon induces a waveguide through the nonlinearity and populates its leaky mode self-consistently. A numerical example of one-dimensional soleakons in a homogeneous medium was demonstrated in Ref. [30]. These soleakons display stable propagation, largely maintaining their intensity profiles for very long propagation distances (orders of magnitude larger than their diffraction lengths). They eventually disintegrate when their localized power decreases to a critical level. It was also shown that soleakons can exhibit coherent and resonance interaction with another faraway soleakon or with the continuum radiation – properties that do not exist in solitons and breathers. In that paper, the soleakon beam induced a double-barrier W structure waveguide which is known to support slowly attenuating leaky modes [31]. The W-shape waveguide was self-induced by combination of nonlocal self-defocusing and local self-focusing nonlinearities. This combination can be realized in optics for example by using nonlocal thermal or molecular reorientational and simultaneously Kerr nonlinearities [32–34]. Beyond optics, Bose Einstein condensate can display simultaneous nonlocal nonlinearity through dipole-dipole interaction and local self-focusing by boson-boson scattering [35, 36]. Still, the requirement for a proper superposition of wide negative and narrow positive nonlinearities is a major restricting factor in the experimental obtainability and impact of soleakons.

Here, we propose and demonstrate numerically two-dimensional soleakons that propagate in arrays of slab wave-guides. Two types of lattice soleakons are predicted: discrete soleakons and Bragg soleakons. Discrete soleakons are supported by combination of nonlocal defocusing and local focusing nonlinearities that jointly induce a ring-barrier wave-guide structure. This waveguide gives rise to slowly-decaying leaky modes that reside within the first band of the lattice transmission spectra. The leakage rate of discrete soleakons increases during propagation. Consequently, they eventually disintegrate abruptly, emitting all their power to delocalized radiation. The predicted Bragg soleakons are supported by local self-focusing nonlinearity only. This means that Bragg soleakons are much more universal than discrete soleakons and soleakons in homogeneous media that require combination of negative nonlocal and positive local nonlinearities. The leakage rate of Bragg soleakons decreases during propagation, hence, Bragg soleakons continue to propagate without disintegration.

The paper is organized as follows. The concept of leaky modes and soleakons is discussed in section 2. The linear transmission spectrum of array of slab wave-guides is analyzed in section 3. The model and methods that we used to find lattice soleakons are presented in section 4. The properties of the discrete and Bragg soleakons are described in section 5. Finally, in section 6 we conclude and suggest directions for future studies.

2. Leaky modes and soleakons

Before moving to lattice soleakons, it is instructive to explain the concept of leaky modes [37] and soleakons in homogeneous media [30]. A leaky mode is localized in the vicinity of the waveguide, exhibiting monotonic decay for a finite distance in a transverse direction, and is oscillatory everywhere beyond that finite distance. During propagation, the localized power in a leaky mode gradually leaks out to the continuum at a constant rate that is given by twice the imaginary part of the mode complex propagation constant. This attenuation rate can be very small, yielding slowly-attenuating leaky modes. Interestingly, the real part of the propagation constant resides within a band of radiation modes. As such, leaky mode is resonant with corresponding radiation modes which comprise its spatial spectrum. In order to excite a leaky

#191503 - $15.00 USD Received 30 May 2013; revised 15 Jul 2013; accepted 15 Jul 2013; published 14 Aug 2013

mode, one has to excite properly its localized section, which resembles a bound state. Because a leaky mode is not a true eigen-mode, the radiation modes comprising it ('in-resonance' radiation modes) dephase, hence radiation is constantly emitted away.

A soleakon induces a waveguide through the nonlinearity and populates its slowly-attenuating leaky mode self-consistently and robustly. Soleakons and their self-induced waveguides are non-stationary because they continuously leak power to the continuum. Self-consistency of soleakon means that during propagation, the localized section of the soleakon beam self-adjusts in such a way that it always fully populates a slowly-attenuating leaky mode of its self-induced waveguide. Importantly, a soleakon should satisfy the above self-consistency condition for propagation distance that is much larger than the diffraction length of the beam under linear propagation condition, L_C. Otherwise, the beam will not exhibit particle-like features such as collisions and therefore cannot be called a soleakon. Like solitons and breathers, soleakons should be stable to noise. Here we explore soleakons in periodic potential: lattice soleakons.

It is worth mentioning that soleakons share some properties with embedded solitons [38–41]: the propagation constants of both entities reside in the continuum spectra of radiation modes. However embedded solitons remain orthogonal to the 'in-resonance' radiation modes during propagation and therefore can be viewed as self-induced bound states in the continuum. In contrast with the embedded solitons, soleakons are self-induced leaky modes that are not orthogonal to the resonant radiation modes and therefore radiate their power to infinity, slowly attenuating during the propagation.

3. Transmission spectrum

All lattice soleakons are nonlinear waves that are trapped by their self-induced defects in periodic potentials. They are universal entities that can be excited in many nonlinear lattices. For concreteness, we analyze optical lattice soleakons in waveguide arrays and use the corresponding terminology. Specifically, we assume a bulk media with linear refractive index change $\Delta n(x,y,z)=\Delta n_0 \cos^2(\pi x/D)$, where $\Delta n_0 = 3\times10^{-3}$ and $D = 3\mu m$ are the amplitude and periodicity of an array of slab sinusoidal waveguides, respectively [Fig. 1(a)]. The linear modes of this structure are given by a product between a one-dimensional Flouqet-Bloch wave in x-axis and a plane wave in y-axis.

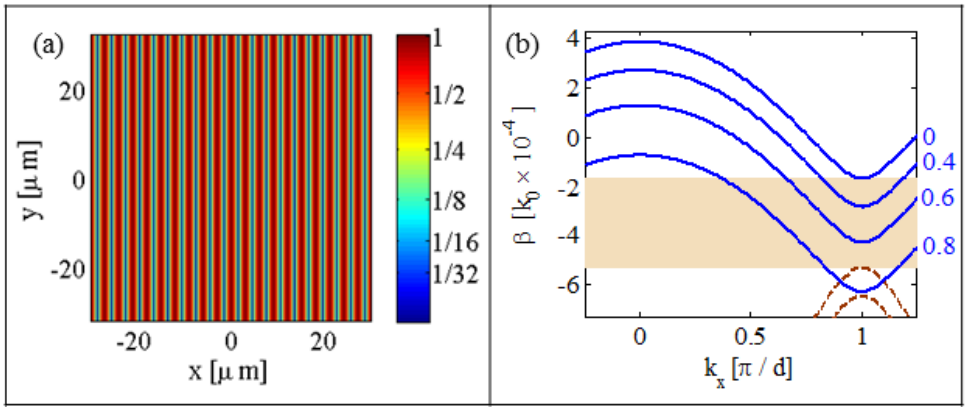

Fig. 1. (a) Refractive index change in the array of slab waveguides. (b) Band structure of the array of slab waveguides. Propagation constants of linear radiation modes of the first (solid blue curves) and second (dash brown curves) band labeled by corresponding values of $k_y D/\pi$. The brown region displays the gap for modes with $k_y = 0$. Radiation modes with $k_y \neq 0$ reside in this gap, forming a semi-infinite band.

#191503 - $15.00 USD Received 30 May 2013; revised 15 Jul 2013; accepted 15 Jul 2013; published 14 Aug 2013

These propagating modes are completely delocalized in both x and y directions. Within the paraxial approximation, the propagation constant of the mode, $\beta_{Bloch}^{q}\left(k_x,k_y\right)$, depends on the Bloch wave-number, k_x, the band number, q and the plane wave wave-number, k_y :

$$\beta_{Bloch}^{q}\left(k_x,k_y\right)=\beta_{Bloch}^{q}\left(k_x,0\right)-k_y^2/2k_0\,, \tag{1}$$

where $k_0=2\pi n_0/\lambda$ is wave-number, $\lambda=0.5\mu m$ is the wave-length of light in vacuum and $n_0=2.2$ is the homogeneous index. Figure 1(b) shows two families of curves representing the propagation constants of the first β_{Bloch}^{1} (solid blue curves) and second β_{Bloch}^{2} (dash brown curves) bands versus k_x for the modes with several k_y *'s*. For a constant k_y, the transmission spectra of the waveguide array is divided into bands that are separated by gaps in which propagating modes do not exist. Such a gap for modes with $k_y=0$ is shown by the brown region in Fig. 1(b). However, as shown in Fig. 1(b), these gaps are full with propagating modes with other k_y *'s*. In other words, the transmission spectrum of our structure consists of a semi-infinite band that is full with propagation waves and a semi-infinite gap above it.

4. Model and methods

Next we consider propagation of a beam in a nonlinear array of slab wave-guides. Such a nonlinear array of slab waveguides can, for example, be optically induced in photorefractives [18, 19] or by periodic voltage biasing in liquid crystals [22]. The complex amplitude, $\psi\left(x,y,z\right)$, of a paraxial beam that propagates in this medium is described by the (2 + 1)D Nonlinear Schrödinger equation:

$$i\frac{\partial\psi}{\partial z}+\frac{1}{2k_0}\nabla_{\perp}^{2}\psi+\frac{k_0}{n_0}\left[\Delta n+\delta n(\psi)\right]\psi=0, \tag{2}$$

where $\delta n(\psi)$ is the nonlinear index change. An approximate solution of Eq. (2) that corresponds to soleakon beam can be written as $\psi_S=A(z)u\left(x,y,z\right)\exp\left(i\beta(z)z\right)$, where $A(z)$ is the peak amplitude, u is the normalized (maximum of u is 1 at every z) slowly-attenuating leaky mode of the structure $\Delta n+\delta n\left(Au\right)$, and $\beta=\beta_R+i\gamma/2$ is the complex propagation constant where $\beta_R\left(z\right)$ and $\gamma\left(z\right)>0$ are real functions with the second corresponding to the leakage rate of the soleakon localized section. Importantly, the beam can be called a soleakon only if it populates slowly attenuating leaky-modes during its propagation such that $1\gg L_C\times\gamma\left(z\right)$ for any z. We now discuss the procedure for finding (lattice) soleakons and verify that they (approximately) solve Eq. (2) [30]. We first calculate the soleakon wave-packet and propagation constant at $z=0$ with a given initial peak amplitude $A\left(0\right)$. For this purpose, we insert $\psi(x,y,z=0)=A(0)u\left(x,y,0\right)\exp\left(i\beta(0)z\right)$ into Eq. (2) and get the following eigen-function problem:

$$\begin{aligned}\beta(0)u(z=0,x,y)&=\frac{1}{2k_0}\nabla_{\perp}^{2}u(z=0,x,y)\\&+\frac{k_0}{n_0}\left\{\Delta n+\delta n\left[A(0)u(z=0,x,y)\right]\right\}u(z=0,x,y),\end{aligned} \tag{3}$$

A slowly-attenuating leaky-modes of Eq. (3) [i.e. $u\left(x,y,z=0\right)$ and $\beta\left(0\right)$] are found numerically by using the self-consistency method for self-induced leaky modes [30]. The

#191503 - $15.00 USD Received 30 May 2013; revised 15 Jul 2013; accepted 15 Jul 2013; published 14 Aug 2013

calculated solution corresponds to a leaky mode of the lattice with the *fixed* defect: $n = n_0 + \Delta n(x,y) + \delta n(A(0)u(z=0,x,y))$. Having found the initial beam, $\psi(x,y,z=0)$, we calculate its nonlinear evolution using two methods that we call "exact" and "adiabatic". In the exact method, we integrated Eq. (2) using split-step Fourier beam propagation method [42]. In the adiabatic method, we integrated Eq. (2) in small steps ($z_m = m \times \Delta z, m = 0,1,2...$), assuming that the beam indeed forms a soleakon, i.e. it self-adjusts such that it always fully populates the slowly-attenuating leaky mode of the self-induced defect. Explicitly, the peak amplitude at $m+1$ step is given by $A(z_{m+1}) = A(z_m)\exp\left[-\gamma(z_m)\Delta z/2\right]$, $u(x,y,z_{m+1})$ and $\beta(z_{m+1})$ are calculated by solving the eigen-function problem [Eq. (3) with $u(x,y,0)$, $A(0)$ and $\beta(0)$ replaced by $u(x,y,z_{m+1})$, $A(z_{m+1})$ and $\beta(z_{m+1})$, respectively]. If the solutions of the exact and adiabatic methods approximately match over propagation distance that is much larger than the diffraction length then it means that the beam is indeed a soleakon. This procedure, which practically follows the definition of (lattice) soleakons, becomes very demanding in terms of computational time for the very large propagation distances that are presented below. In these cases, we used the equation for evolution of peak intensity of the beam in adiabatic approximation

$$dA/dz = -\gamma(A)\,A(z), \tag{4}$$

where the momentary leakage rates for each waveguide realization, $\gamma(A)$, were calculated by finding M leaky-mode solutions of Eq. (3) with different peak amplitudes $A_m, m = 1...M$. Function $\gamma(A)$ was evaluated by fitting M_{th} order polynomial to the M values of leakage rates $\gamma(A_m)$. Then, $A(z)$ was found by numerically solving Eq. (4) with $\gamma(A)$ and $A(0)$ equal to the peak intensity of initial beam in the exact beam propagation method. The peak intensity found by such method was compared to the one from the exact beam propagation method over propagation distance that is much larger than the diffraction length.

5. Discrete and Bragg soleakons

Next we present our results for lattice soleakons, starting with discrete soleakons. In contrast to discrete solitons that reside in the semi-infinite gap, propagation constant of discrete soleakons must be "shifted" downward into the first band. This condition can be obtained by combination of nonlocal self-defocusing and localized self-focusing [30]. Here, we assume the following nonlinearity $\delta n = \delta n_1 |\psi|^2 / \left(1 + \varsigma |\psi|^2\right) - \delta n_2 / \sigma^2 \int_{-\infty}^{+\infty} d\eta \int_{-\infty}^{+\infty} d\xi \left\{ |\psi[x-\xi, y-\eta]|^2 \exp\left[-\left(\eta^2 + \xi^2\right)/\sigma^2\right]\right\}$, where $\delta n_1 = 6\times10^{-8}\ cm^2/W$ and $\delta n_2 = 1.2\times10^{-6}\ cm^2/W$ are strengths of the saturable self-focusing and nonlocal defocusing nonlinearities, respectively, $\varsigma = 5\times10^{-5}\ cm^2/W$ is saturation coefficient and $\sigma = 30\mu m$ is nonlocality range. We start with determining the initial peak intensity $|A(0)|^2 = 4\times10^4\ W/cm^2$ and find the initial beam by solving Eq. (3) [its intensity is shown in Fig. 2(a)]. The power of the localized component $P_{localized}$, which we define by $P_{localized} = \int_{-\infty}^{+\infty} dx \int_{-\infty}^{+\infty} dy |\psi(x,y)|^2 H\left[|\psi(x,y)|^2 / |A|^2 - 0.01\right]$, where $H(x)$ is Heaviside step function, is $5.6mW$. Next, we propagated the initial beam in a linear lattice by solving Eq. (2) with $\delta n = 0$ from which we estimate the diffraction length to be $L_C = 0.016cm$ [Fig. 2(b) shows the intensity at $z = 0.032cm = 2 \times L_C$]. We then calculated the nonlinear evolution of the initial beam using the 'exact' method. The intensity patterns at $z = 107cm$ ($\approx 6700 \times L_C$) and

#191503 - $15.00 USD Received 30 May 2013; revised 15 Jul 2013; accepted 15 Jul 2013; published 14 Aug 2013

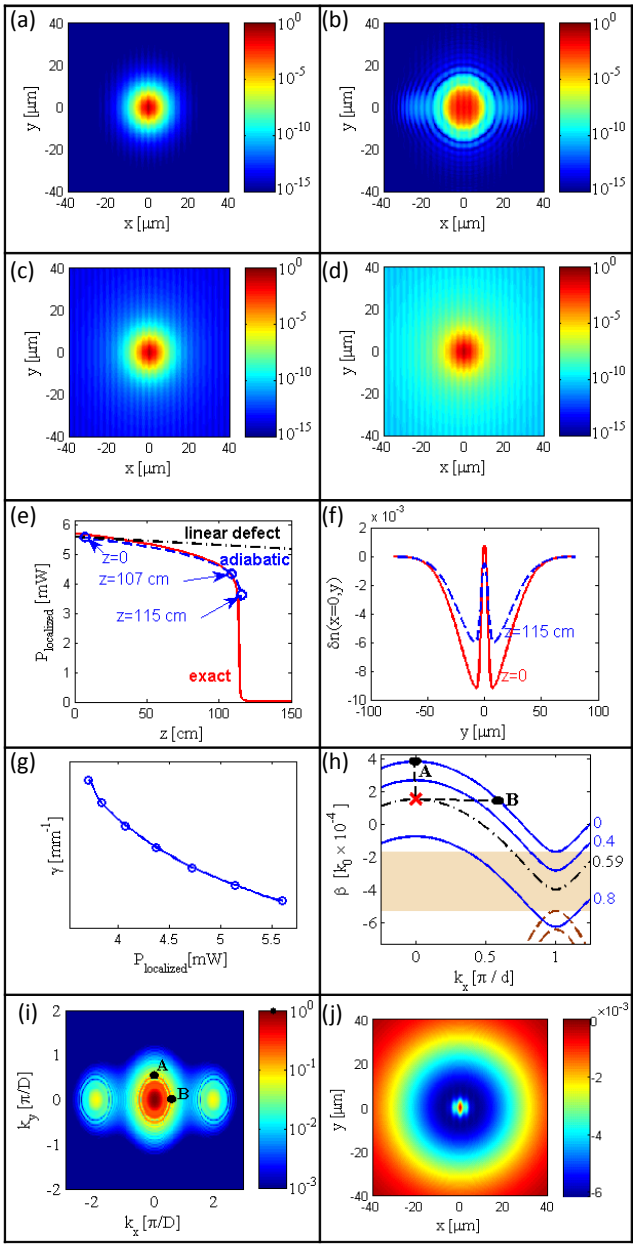

Fig. 2. (a) Intensity profile of discrete soleakon at z = 0 (logarithmic scale); (b) Intensity profile of beam in a linear lattice ($\delta n = 0$) at z = 0.032cm = 2 × L_C; Intensity profiles of soleakon (logarithmic scale) at z = 107cm (c) and at z = 115cm (d); (e) localized power versus propagation distance obtained by adiabatic (blue dashed curve) and exact (red solid curve) methods and for linear defect (black dash-dot curve). The input beam in the exact method corresponded to 1.0125 times the input beam in the adiabatic method; (f) Nonlinear defect vs. y in the x = 0 cross section at z = 0 (red solid curve) and z = 115cm (blue dashed curve); (g) Soleakon decay rate versus localized power; (h) Propagation constant of the discrete soleakon (red cross) on the background of linear band structure. The propagation constant of the soleakon is shifted from the upper edge of the first band downward into the first band; (i) Fourier power spectrum of the discrete soleakon wave-function (logarithmic scale). Narrow rings around the humps correspond to the radiation part of the soleakon; (j) Ring-barrier waveguide induced by local focusing and nonlocal defocusing nonlinearities.

#191503 - $15.00 USD Received 30 May 2013; revised 15 Jul 2013; accepted 15 Jul 2013; published 14 Aug 2013

$z = 115cm$ ($\approx 7200 \times L_C$) are shown in Figs. 2(c) and 2(d), respectively, showing that while the beam somewhat broadened, it stayed localized for propagation distance that is many times larger than the diffraction length. We then calculated the evolution of the initial beam using the adiabatic method and verify that it matches very well to the evolution using the exact method. Thus, we conclude that the beam is indeed a soleakon. This matching is displayed in Fig. 2(e) that shows the calculated localized power using the exact and adiabatic methods. Figure 2(e) also shows the localized power when the initial beam propagates linearly in a fixed defect that corresponds to the self-induced defect at $z = 0$ [its cross section is shown in Fig. 2(f)]. As shown, the soleakon beam attenuates faster than in the linear case. Eventually it disintegrates abruptly emitting all its localized power to the continuum. This type of dynamics was also observed for soleakons in homogeneous media [30]. It results from the fact that the leakage rate of this leaky mode increases with decreasing localized power [Fig. 2(g)] because the defect gets shallower and narrower [Fig. 2(f)]. Figures 2(h)-2(j) display properties of the self-induced leaky modes (the soleakon at $z = 115cm$). The real part of the soleakon propagation constant [red cross in Fig. 2(h)] resides within the first band. The beam power spectrum [Fig. 2(i)] consists of intense humps that correspond to the localized section and thin lines around them that are associated with the conical radiation. Finally, Fig. 2(j) shows the induced ring-barrier waveguide structure which is the 2D version of the 1D double-barrier waveguide which is known to support slowly-attenuating leaky modes.

The discrete soleakons in the array of slab wave-guides presented above are similar to the soleakons in homogeneous media [30] in that they both require a combination of nonlocal defocusing with local focusing nonlinearities and decay at increasing rate during propagation. Next, we show Bragg soleakons that exhibit properties that are profoundly different from those of the homogeneous and discrete soleakons. Bragg soleakons do not require the combination of nonlocal defocusing with local focusing nonlinearities and can be realized in array of slab waveguides with only saturable self-focusing. Propagation constants of these soleakons are shifted from the upper edge of the second band upward into the semi-infinite continuum of the first band. They radiate power into specific angles and decay at a decreasing rate and therefore do not disintegrate.

To find Bragg soleakons we assumed the following nonlinearity $\delta n = \delta n_1 |\psi|^2 / \left(1 + \varsigma |\psi|^2\right)$, where $\delta n_1 = 10^{-7}\, cm^2/W$ is strength of saturable self-focusing nonlinearity and $\varsigma = 8 \times 10^{-5}\, cm^2/W$ is saturation coefficient. We start with determining the initial peak intensity $|A(0)|^2 = 2.8 \times 10^4\, W/cm^2$ and find the initial beam as localized eigen-function of Eq. (3) whose eigen-value is shifted from the upper edge of the second band upward into the first band. The initial intensity profile of the Bragg soleakon is presented in Fig. 3(a). The power of the localized component (defined above) is $P_{localized} = 10mW$. The diffraction length was estimated by linear propagation of initial beam which was modeled by solving Eq. (2) with $\delta n = 0$ [Fig. 3(b) shows the intensity at $z = 0.05cm = 2 \times L_C$]. The nonlinear propagation of the beam was than evaluated using the 'exact' method. The intensity patterns at $z = 8cm$ ($\approx 320 \times L_C$) and $z = 50cm$ ($\approx 2000 \times L_C$) [Figs. 3(c) and 3(d), respectively] show that, similarly to the Discrete soleakon, Bragg soleakon broadens but stays localized for propagation distance that is many times larger than the diffraction length.

#191503 - $15.00 USD Received 30 May 2013; revised 15 Jul 2013; accepted 15 Jul 2013; published 14 Aug 2013

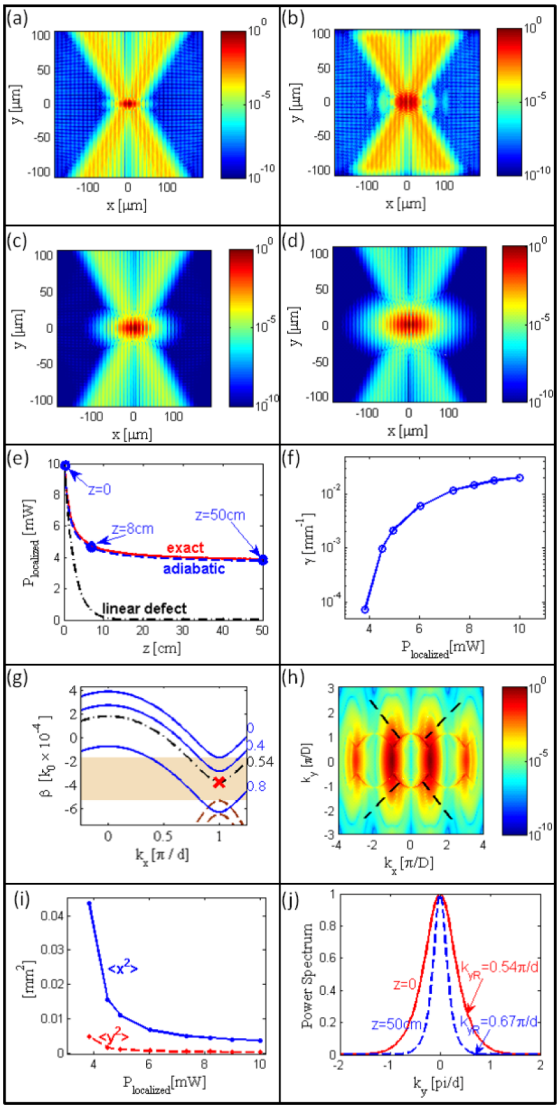

Fig. 3. (a) Intensity profile of Bragg soleakon at $z = 0$ (logarithmic scale); (b) Intensity profile of beam in a linear lattice ($\delta n = 0$) at $z = 0.05cm = 2 \times L_C$; Intensity profiles of soleakon (logarithmic scale) at $z = 8$ (c) and at $z = 50cm$ (d); (e) localized power versus propagation distance obtained by adiabatic (blue dashed curve) and exact (red solid curve) methods and for linear defect (black dash-dot curve). (f) Soleakon decay rate versus localized power; (g) Propagation constant of the Bragg soleakon (red cross) on the background of linear band structure. The propagation constant of the soleakon is shifted from the upper edge of the second band upward into the first band; (h) Fourier power spectrum of the Bragg soleakon wave-function (logarithmic scale). Narrow lines connecting hot-spots correspond to the radiation part of the soleakon. Normals (black dashed lines) point in the direction of radiation; (i) Soleakon widths $\left\langle x^2 \right\rangle = \int_{-\infty}^{+\infty} dx \int_{-\infty}^{+\infty} dy \; x^2 \left|\psi(x,y)\right|^2 \Big/ \left|\psi\right|^2_{\max}$ (blue solid curve) and $\left\langle y^2 \right\rangle = \int_{-\infty}^{+\infty} dx \int_{-\infty}^{+\infty} dy \; y^2 \left|\psi(x,y)\right|^2 \Big/ \left|\psi\right|^2_{\max}$ (red dashed curve) versus localized power; (j) Fourier power spectrum of the soleakon wave-function vs. k_y at $k_x = \pi / d$ and $z = 0$ (red solid curve) and $z = 50cm$ (blue dashed curve). Arrows point to the minimal values of resonant plane wave-numbers k_{yR}.

#191503 - $15.00 USD Received 30 May 2013; revised 15 Jul 2013; accepted 15 Jul 2013; published 14 Aug 2013

We then calculated the evolution of the initial beam using the adiabatic method. Figure 3(e) shows the localized power vs. the propagation distance obtained by exact (blue dashed curve) and adiabatic (red solid curve) methods. The fine matching between two methods confirms that the beam is indeed a soleakon. Black dash-dot curve in Fig. 3(e) represents the localized power when the initial beam propagates linearly in a fixed defect that corresponds to the self-induced defect at $z = 0$. As shown the Bragg soleakon attenuates slower than the linear case and continues to propagate without disintegration. This results from the fact that the leakage rate of the Bragg soleakon decreases with localized power [Fig. 3(f)]. Figures 3(g)-3(h) display properties of the self-induced leaky modes corresponding to Bragg soleakon at $z = 0$. Real part of its propagation constant $\mathrm{Re}\left(\beta_{Soleakon}\right)$ [red cross in Fig. 3(g)] resides in the region filled by radiation modes from the first band with nonzero k_y. Its power spectrum [Fig. 3(h)] consists of intense humps that correspond to the localized section and thin lines between them, which correspond to the radiation part of the soleakon. The two most intense humps are centered around $k_x = \pm\pi/D,$ because Bragg soleakon bifurcates from the upper edge of the second band and hence is Bragg-matched with the lattice.

Next, we explain the differences in the radiation patterns of the lattice soleakons (conical in all directions in discrete versus bow-tie shaped into specific angles in Bragg soleakons) and longitudinal dynamics of their decay rates (increasing in discrete while decreasing in Bragg soleakons). Radiation into the narrow region in k space [thin lines in Fig. 2(i) and 3(h)] results from the resonance condition between soleakon and radiation modes $\beta^1_{Bloch}\left(k_x, k_{yR}\right) = \beta_R,$ where k_{yR} is plane-wave wave-number, of the "in-resonance" radiation modes. Substituting Eq. (1) into the this expression, one finds that these lines are given by

$$k_{yR} = \pm\sqrt{2k_0\left[\beta^1_{Bloch}\left(k_x, k_y = 0\right) - \beta_R\right]}. \tag{5}$$

The slope of these lines is given by

$$\pm\left(k_0 \big/ \left|k_{yR}\right|\right)\left(\partial\beta^1_{Bloch}\left(k_x, k_y = 0\right)\big/\partial k_x\right). \tag{6}$$

In discrete soleakons [Fig. 2(i)], this slope changes from 0 [point A in Figs. 2(h) and 2(i)] to infinity [point B in Fig. 2(h) and 2(i)]. Therefore the normals to these curves cover 2π angle. The directions of these normals correspond to the directions of the power radiation in real space. Thus, discrete soleakons radiate power to all directions. For Bragg soleakons, the real part of propagation constant is smaller than propagation constant of first band radiation modes with $k_y = 0$ $\beta^1_{Bloch}\left(k_x, k_y = 0\right) > \beta_R$ [see Fig. 3(g)]. Hence resonance condition [Eq. (5)] requires that the plane wave-numbers of the "in-resonance" radiation modes k_{yR} lie outside the band given by $\left|k_{yR}\right| > \sqrt{2k_0\left[\beta^1_{Bloch}\left(k_x, k_y = 0\right) - \beta_R\right]}$. Therefore the slope of the lines in its power spectrum [Fig. 3(h)], given by Eq. (6), is finite, and the normals to these lines cover the specific angles in the upper and lower half planes of the Fourier space as shown by black dashed lines in Fig. 3(h). The directions of these normals correspond to the directions of the power radiation in real space. Therefore Bragg soleakons radiate power into the specific angles, which is reflected by the characteristic bow-tie shape of the radiation pattern [Figs. 3(a)-3(d)]. In contrast with the discrete soleakons, Bragg soleakons decay at a decreasing rate and continue to propagate without disintegration. This is related to the fact that in Bragg soleakons, the spatial width of its localized section increases and its bandwidth decreases as a result of the decrease in soleakon localized power [Figs. 3(i) and 3(j)]. It follows from the resonance condition [Eq. (5)] that only the tails of its spectrum with $\left|k_y\right| > \sqrt{2k_0\left[\beta^1_{Bloch}\left(k_x, k_y = 0\right) - \beta_R\right]}$ belong to the radiation modes [Fig. 3(j)]. Therefore the

#191503 - $15.00 USD Received 30 May 2013; revised 15 Jul 2013; accepted 15 Jul 2013; published 14 Aug 2013

band-width decrease results in the reduction of the radiative fraction of its spectrum [blue dashed curve in Fig. 3(j)] and hence in the weaker radiation and smaller decay rate of the soleakon.

6. Conclusion

In conclusions, we predicted and demonstrated numerically lattice soleakons (discrete and Bragg): robust self-trapped leaky waves that induce defects in the lattice and populate their leaky modes (resonance states) self-consistently. Lattice soleakons exhibit stable propagation, largely maintaining their intensity profiles, for very long propagation distances (orders of magnitude larger than their diffraction lengths). We anticipate that lattice soleakons will be experimentally demonstrated in several physical systems, including optics and Bose Einstein condensates. Importantly, the fact that Bragg soleakons are supported by only local self-focusing nonlinearity significantly extends the range of physical systems in which soleakons exist and can be explored experimentally. In this respect, Bragg soleakons are probably more universal than discrete soleakons or the homogeneous soleakons of Ref. [30]. We also expect that lattice soleakons can exhibit wealth of intrinsic dynamics (e.g. multi-mode vector soleakons and incoherent soleakons) and of extrinsic dynamics (e.g. moving and accelerating soleakons). The fact that soleakons interact strongly and selectively with radiation modes and with other soleakons, that are possibly far away, may give rise to new phenomena and applications that do not exist with lattice solitons.

Acknowledgments

We acknowledge the support of the I-CORE Program of the Planning and Budgeting Committee and The Israel Science Foundation.

#191503 - $15.00 USD Received 30 May 2013; revised 15 Jul 2013; accepted 15 Jul 2013; published 14 Aug 2013